Video-rate dual polarization multispectral endoscopic imaging

Anne Pigula[a,b]*, Neil T. Clancy[a,b], Shobhit Arya[b] George B. Hanna[b], Daniel S. Elson[a,b]
[a]Hamlyn Centre for Robotic Surgery, Institute of Global Health Innovation, Imperial College London, SW7 2AZ, UK; [b]Department of Surgery and Cancer, Imperial College London, SW7 2AZ, UK, * Current address: Harvard-Massachusetts Institute of Technology Division of Health Sciences and Technology, Cambridge, Massachusetts USA

ABSTRACT

Cancerous and precancerous growths often exhibit changes in scattering, and therefore depolarization, as well as collagen breakdown, causing changes in birefringent effects. Simple difference of linear polarization imaging is unable to represent anisotropic effects like birefringence, and Mueller polarimetry is time-consuming and difficult to implement clinically. This work presents a dual-polarization endoscope to collect co- and cross-polarized images for each of two polarization states, and further incorporates narrow band detection to increase vascular contrast, particularly vascular remodeling present in diseased tissue, and provide depth sensitivity. The endoscope was shown to be sensitive to both isotropic and anisotropic materials in phantom and *in vivo* experiments.

Keywords: Polarization, polarimetry, anisotropy, multispectral, NBI, endoscopy

1. INTRODUCTION

In recent years, polarization imaging has emerged as an important tool for studying structural properties in biological tissue. In its simplest form, polarization imaging involves comparing co-polarized (CO) and cross-polarized (CR) images in a metric called the Degree of Linear Polarization (DoLP):

$$DoLP = \frac{CO-CR}{CO+CR} \quad (1)$$

DoLP imaging is an attractive modality for clinical implementation because it can be performed quickly and with simple instrumentation. However, the DoLP is unable to differentiate depolarization from anisotropic responses like diattenuation, birefringence, or retardance[1]. In contrast, Mueller polarimetry fully describes the polarization properties of a sample in terms of depolarization, diattenuation and retardance. However, the acquisition of at least sixteen unique images is both time-consuming and mechanically difficult to implement even when using cameras that can record multiple states in parallel, and as a result clinical adaptation is challenging.

To address the gap between DoLP imaging and Mueller polarimetry, Morgan *et al*. proposed Rotating Orthogonal Polarization Imaging (ROPI), in which CR images for two orthogonal polarization states are compared using a normalized difference similar to the DoLP calculation[2]. Their main result is the elimination of surface reflections which may overpower the signal from embedded targets, but they acknowledge that without CO data their system will be unable to accurately represent birefringence[3]. Several other systems have been developed which extract a measure of anisotropy from a target, but these generally do not meet the time or space constraints of clinical use[4,5].

It is of additional value to consider narrow band imaging (NBI) to obtain vascular highlighting and depth-gated measurements. Green and blue light penetrate shallowly, where they provide good contrast of capillaries, and longer-wavelength red light allows deeper imaging of larger subsurface vessels. Comparing the reflectance of tissue at blue/green wavebands with respect to red provides sharp contrast of capillary beds, highlights areas of increased vasculature, and can indicate the depth of a feature.

A polarized stereo endoscope with NBI capabilities previously developed by this lab[6] was adapted to alternate between two illumination polarization states, allowing enhanced optical characterization of tissue and determination of system isotropy.

2. MATERIALS AND METHODS

2.1 System design

The endoscopic system was similar to one described previously[6], but utilized a stereo endoscope with two distinct light channels (Figure 1) (Intuitive Surgical Inc., Sunnyvale, USA). A custom linear polarization filter was constructed from high contrast linear polarizers (FPC-12.5-475-625, CVI Melles Griot, Albuquerque, USA) to polarize one illumination/imaging pair orthogonally (90±1.5°) to the other pair to achieve generation and detection of two polarization states, here called the H- and V-states (Fig. 1). An optical chopper alternated between these illumination states allowing acquisition of both CO and CR images for each of two incident polarization states.

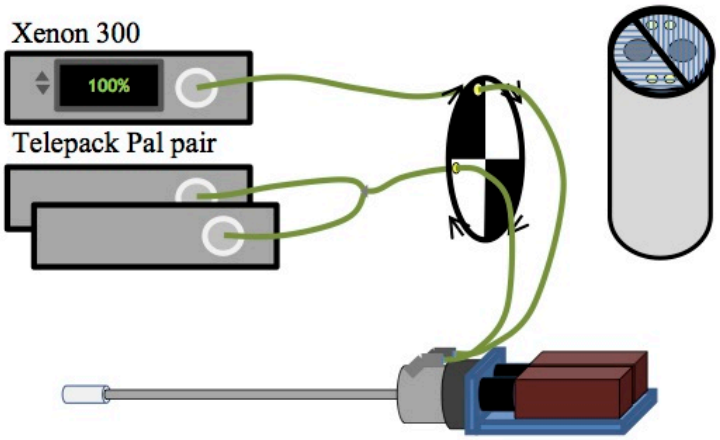

Figure 1. (left) Broadband white light sources were alternated using a light chopper and then coupled to the endoscope. Two high speed cameras were mounted at the base of the endoscope to capture the targeted images. (right) A custom polarizing window was fitted to the distal end of the scope. Each half of the window covered one imaging channel and one illumination channel.

2.2 Validation tests

A series of optical phantoms were imaged for initial system validation. A paper towel was used to model diffuse reflection of light, and a metal washer secured to a piece of white paper was used to produce an isotropic polarization-maintaining specular reflection. A linear polarizer, a simple model of diattenuation, was secured to a piece of white paper, a diffuse reflector, with the transmission axis marked on the paper. The polarizer was rotated to acquire images at a number of orientations.

An *in vivo* proof of concept study was carried out on a porcine subject (45 kg female domestic white pig) undergoing an investigative abdominal procedure. Multiple image sets were taken to account for motion artifact or other acquisition errors, and anatomical features were identified by the surgeon both during acquisition and after analysis.

2.3 Post-processing algorithm

A multi-step processing algorithm corrected unwanted inter-image differences and extracted structural information about the target. After blur corrections, color adjustments, and registration, image sets could be directly compared to extract structural information. A vascular map was calculated by normalizing the difference between R and G images by the summed R and G intensities. The DoLP was calculated to extract polarization information, followed by a histogram equalization in each color channel to improve contrast.

A novel analysis metric was developed in this work to indicate the degree and orientation of anisotropy. The Degree of Alignment (DoA) is similar to the ROPI polarization ratio[2], but compares the sum of direct reflection and scattering rather than scattered light alone.

$$DoA = \frac{CO_H - CO_V}{CO_H + CO_V} \quad (2)$$

The DoA calculation was designed to indicate the orientation of the transmission axis of a linearly polarizing filter and indicated preferential absorption of H or V-state light. In biological tissue, which is more likely to depolarize or retard light, a positive DoA signal indicates a higher level of direct, unscattered reflection for H-state illumination and a negative DoA indicates a higher level of direct, unscattered reflection for V-state illumination.

3. RESULTS

3.1 Optical phantoms

The DoLP measurements of the diffuse reflector are uniformly low at both illumination states due to the isotropically depolarizing behavior of the model. In certain regions, textural qualities are visible that give a dappled effect. This could result from registration errors, but more likely indicates that paper towel is not perfectly depolarizing and there is a low level of direct reflection highlighting variations in the surface topology.

In the case of the specular reflector, the direct reflection is clearly visible in both CO images with some variations due to differences in illumination source location, and the washer appears nearly black in both CR images. As expected from an isotropic phantom, the DoLP signal is high at areas of reflection and low for the diffusely reflecting background, and equivalent for both illumination states.

The linear polarizer transmits light when the transmission axis of the target filter is aligned with the illumination state. When this is true the DoLP is 1, and when the illumination state and filter axis are orthogonal, the DoLP is 0. When the target filter fully transmits light for one illumination state, it attenuates the other illumination state. The DoA indicates, for a given rotation of the target filter, its similarity to each illumination state. When the filter axis is approximately aligned with H-state illumination axis, the DoA is near +1. When the filter is rotated so its axis is approximately aligned with V-state illumination, the DoA is near -1.

3.2 *In vivo* validation

Figure 2a shows a total intensity image (CO+CR) from the porcine test with several different materials in the field of view. The small intestine runs horizontally across the image, with an unidentified organ (likely a different segment of the small intestine) below and behind it. Gauze is visible below and to the right of the small intestine. Blood vessels and mesenteric fat extend from the small intestine towards the top left corner of the image.

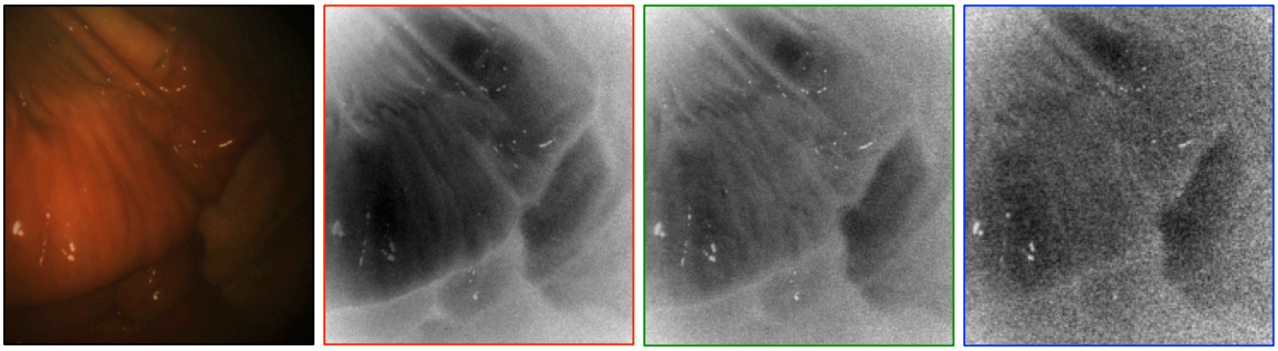

Figure 2: (a) Total intensity image featuring the small intestine, gauze, mesenteric fat, and blood vessels. (b-d) From left to right, DoLP maps in the red, green, and blue channels

Gauze and fat are both strongly scattering materials, and in the DoLP maps (Figure 2b-d), these regions have low values due to their depolarizing behavior. In contrast, the blood vessels in the top left corner are strong absorbers. They present a high DoLP value because the photons that have penetrated into the vessels are typically absorbed before they can scatter back to the detector.

The system attenuated light throughput and increased noise levels at shorter wavelengths, most noticeably in the blue channel. Despite this, the DoLP of the small intestine is higher and has greater contrast in the blue and green channels than the red channel. This is due to the presence of hemoglobin and other absorbers that preferentially absorb short-wavelength blue and green light, resulting in a higher rate of re-emission of scattered photons in the red band and therefore a lower DoLP.

4. DISCUSSION AND CONCLUSIONS

Both phantom and *in vivo* results suggest real value for this system in a clinical setting. Phantom validation tests confirm the system's ability to increase contrast based on structural properties, namely the target's depolarizing behavior. Additionally, the DoA compares CO data from two illumination states to assess the target's isotropy. In a porcine test, the system was able to differentiate multiple targets, including small intestine, fat, blood vessels, and gauze.

To validate the system in a human pathological test, *ex vivo* studies using the multispectral dual polarization imaging system are in progress of healthy, cystic, endometriotic, and cancerous human ovarian tissue samples.

ACKNOWLEDGEMENTS
Funding for this work was provided by ERC grant 242991, NIHR (HTD240), UK EPSRC grant EP/E06342X/1, an Intuitive Surgical Technology Research grant, and the Imperial NIHR Biomedical Research Centre. Anne Pigula gratefully acknowledges the financial support of a Whitaker Fellowship. Neil Clancy gratefully acknowledges the financial support of an Imperial College Junior Research Fellowship. The authors would like to thank the Northwick Park Institute for Medical Research for assistance with the surgical trial arrangements.

5. REFERENCES

[1] Sankaran, V., Everett, M. J., Maitland, D. J., and Walsh, J. T., "Comparison of polarized-light propagation in biological tissue and phantoms," Optics Letters 24(15), 1044-1046 (1999).
[2] Morgan, S.P., Zhu, Q., Stockford, I. M., and Crowe, J. A., "Rotating orthogonal polarization imaging," Optics Letters 33(13), 1503-1505 (2008).
[3] Zhu, Q., Stockford, I. M., Crowe, J. A., and Morgan, S. P., "Experimental and theoretical evaluation of rotating orthogonal polarization imaging," Journal of Biomedical Optics 14(3), 034006-034006-10 (2009).
[4] Nan, Z., Xiaoyu, J., Qiang, G., Yonghong, H., and Hui, M., "Linear polarization difference imaging and its potential applications," Applied Optics 48(35), 6734-6739 (2009).
[5] Wallenburg, M.A., Wood, M. F. G., Ghosh, N., and Vitkin, I. A., "Polarimetry-based method to extract geometry-independent metrics of tissue anisotropy," Optics Letters 35(15), 2570-2572 (2010).
[6] Clancy, N.T., Arya, S., Qi, J., Stoyanov, D., Hanna, G. B., and Elson, D. S., "Polarised stereo endoscope and narrowband detection for minimal access surgery," Biomed. Opt. Express 5, 4108-4117 (2014).